

Phase-sensitive correlation optical time-domain reflectometer using quantum phase noise of laser light

A. Arias,¹ M.G. Shlyagin,^{1,*} S.V. Miridonov,¹ and Rodolfo Martinez Manuel^{2,3}

¹Department of Optics, Center for Scientific Research and Higher Education of Ensenada (CICESE), carretera Ensenada-Tijuana 3918, Ensenada, B.C. 22860 Mexico

²Centro de Investigaciones en Óptica, A.C. Photonics, Prol. Constitución 607, Fracc. Reserva Loma Bonita Aguascalientes, 20200, Mexico

³Electrical and Electronic Engineering Science Department, University of Johannesburg, Auckland Park 2006, South Africa

*mish@cicese.mx

Abstract: We propose and experimentally demonstrate a simple approach to realize a phase-sensitive correlation optical time-domain reflectometer (OTDR) suitable for detection and localization of dynamic perturbations along a single-mode optical fiber. It is based on the quantum phase fluctuations of a coherent light emitted by a telecom DFB diode laser. Truly random probe signals are generated by an interferometer with the optical path difference exceeding the coherence length of the laser light. Speckle-like OTDR traces were obtained by calculating cross-correlation functions between the probe light and the light intensity signals returned back from the sensing fiber. Perturbations are detected and localized by monitoring time variations of correlation amplitude along the fiber length. Results of proof-of-concept experimental testing are presented using an array of ultra-low-reflectivity fiber Bragg gratings as weak reflectors.

©2015 Optical Society of America

OCIS codes: (060.2300) Fiber measurements; (060.2370) Fiber optic sensors; (120.4825) Optical time domain reflectometry.

References and links

1. J. H. Cole, J. A. Bucaro, C. K. Kirkendall, and A. Dandridge, "The origin, history and future of fiber-optic interferometric acoustic sensors for US Navy applications," *Proc. SPIE* **7753**, 775303 (2011).
2. J. P. Dakin, D. A. Pearce, C. A. Wade, and A. Strong, "A novel distributed optical fibre sensing system enabling location of disturbances in a Sagnac loop interferometer," *Proc. SPIE* **838**, 325–328 (1988).
3. E. Udd, "Sagnac distributed sensor concepts," *Proc. SPIE* **1586**, 46–52 (1992).
4. S. J. Russell, K. R. C. Brady, and J. P. Dakin, "Real-time location of multiple time-varying strain disturbances, acting over a 40-km fiber section, using a novel dual-Sagnac interferometer," *J. Lightwave Technol.* **19**(2), 205–213 (2001).
5. R. M. Manuel, M. G. Shlyagin, and S. V. Miridonov, "Location of a time-varying disturbance using an array of identical fiber-optic interferometers interrogated by CW DFB laser," *Opt. Express* **16**(25), 20666–20675 (2008).
6. J. C. Juarez, E. W. Maier, K. N. Choi, and H. F. Taylor, "Distributed fiber optic intrusion sensor system," *J. Lightwave Technol.* **23**(6), 2081–2087 (2005).
7. Y. Lu, T. Zhu, L. Chen, and X. Bao, "Distributed vibration sensor based on coherent detection of phase-OTDR," *J. Lightwave Technol.* **28**(22), 3243–3249 (2010).
8. F. Peng, H. Wu, X.-H. Jia, Y. J. Rao, Z. N. Wang, and Z. P. Peng, "Ultra-long high-sensitivity Φ -OTDR for high spatial resolution intrusion detection of pipelines," *Opt. Express* **22**(11), 13804–13810 (2014).
9. H. Izumita, Y. Koyamada, S. Furukawa, and I. Sankawa, "The performance limit of coherent OTDR enhanced with optical fiber amplifiers due to optical nonlinear phenomena," *J. Lightwave Technol.* **12**(7), 1230–1238 (1994).
10. H. F. Martins, S. Martin-Lopez, P. Corredera, P. Salgado, O. Frazão, and M. González-Herráez, "Modulation instability-induced fading in phase-sensitive optical time-domain reflectometry," *Opt. Lett.* **38**(6), 872–874 (2013).
11. Z. N. Wang, J. J. Zeng, J. Li, M. Q. Fan, H. Wu, F. Peng, L. Zhang, Y. Zhou, and Y. J. Rao, "Ultra-long phase-sensitive OTDR with hybrid distributed amplification," *Opt. Lett.* **39**(20), 5866–5869 (2014).

12. Z. N. Wang, J. Li, M. Q. Fan, L. Zhang, F. Peng, H. Wu, J. J. Zeng, Y. Zhou, and Y. J. Rao, "Phase-sensitive optical time-domain reflectometry with Brillouin amplification," *Opt. Lett.* **39**(15), 4313–4316 (2014).
13. T. Zhu, Q. He, X. Xiao, and X. Bao, "Modulated pulses based distributed vibration sensing with high frequency response and spatial resolution," *Opt. Express* **21**(3), 2953–2963 (2013).
14. Q. He, T. Tao Zhu, X. Xiao, B. Zhang, D. Diao, and X. Bao, "All fiber distributed vibration sensing using modulated time-difference pulses," *IEEE Photon. Technol. Lett.* **25**(20), 1955–1957 (2013).
15. H. F. Martins, S. Martin-Lopez, P. Corredera, M. L. Filograno, O. Frazão, and M. González-Herráez, "Phase-sensitive optical time domain reflectometer assisted by first-order Raman amplification for distributed vibration sensing over >100 km," *J. Lightwave Technol.* **32**(8), 1510–1518 (2014).
16. W. Eickhoff and R. Ulrich, "Optical frequency domain reflectometry in single-mode fiber," *Appl. Phys. Lett.* **39**(9), 693–695 (1981).
17. D. Uttam and B. Culshaw, "Precision time domain reflectometry in optical fiber systems using frequency modulated continuous wave ranging technique," *J. Lightwave Technol.* **3**(5), 971–977 (1985).
18. M. Nazarathy, S. A. Newton, R. P. Giffard, D. S. Moberly, F. Sischka, W. R. Trutna, Jr., and S. Foster, "Real-time long range complementary correlation optical time domain reflectometer," *J. Lightwave Technol.* **7**(1), 24–38 (1989).
19. D. Arbel and A. Eyal, "Dynamic optical frequency domain reflectometry," *Opt. Express* **22**(8), 8823–8830 (2014).
20. K. Okada, K. Hashimoto, T. Shibata, and Y. Nagaki, "Optical cable fault location using correlation technique," *Electron. Lett.* **16**(16), 629–630 (1980).
21. M. Zoboli and P. Bassi, "High spatial resolution OTDR attenuation measurements by a correlation technique," *Appl. Opt.* **22**(23), 3680–3681 (1983).
22. Y. Wang, B. Wang, and A. Wang, "Chaotic correlation optical time domain reflectometer utilizing laser diode," *IEEE Photon. Technol. Lett.* **20**(19), 1636–1638 (2008).
23. Z. N. Wang, M. Q. Fan, L. Zhang, H. Wu, D. V. Churkin, Y. Li, X. Y. Qian, and Y. J. Rao, "Long-range and high-precision correlation optical time-domain reflectometry utilizing an all-fiber chaotic source," *Opt. Express* **23**(12), 15514–15520 (2015).
24. M. G. Shlyagin and A. Arias, "Simple CW correlation OTDR for interrogation of multiplexed low-reflectivity FBG sensors," *Proc. SPIE* **7753**, 77538V (2011).
25. M. G. Shlyagin, A. Arias, and R. Manuel Martinez, "Distributed detection and localization of multiple dynamic perturbations using coherent correlation OTDR," *Proc. SPIE* **9157**, 91576Z (2014).
26. P. B. Gallion and G. Debarge, "Quantum phase noise and field correlation in single frequency semiconductor laser systems," *J. Quant. Electron.* **20**(4), 343–349 (1984).
27. B. Moslehi, "Analysis of optical phase noise in fiber-optic systems employing a laser source with arbitrary coherence time," *J. Lightwave Technol.* **4**(9), 1334–1351 (1986).
28. H. Guo, W. Tang, Y. Liu, and W. Wei, "Truly random number generation based on measurement of phase noise of a laser," *Phys. Rev. E Stat. Nonlin. Soft Matter Phys.* **81**(5), 051137 (2010).
29. F. Xu, B. Qi, X. Ma, H. Xu, H. Zheng, and H.-K. Lo, "Ultrafast quantum random number generation based on quantum phase fluctuations," *Opt. Express* **20**(11), 12366–12377 (2012).
30. H. D. Hinkley and C. Freed, "Direct observation of the Lorentzian line shape as limited by quantum phase noise in a laser above threshold," *Phys. Rev. Lett.* **23**(6), 277–280 (1969).

1. Introduction

Distributed fiber-optic sensors have a unique distinctive advantage of capability to perform simultaneous measurements in thousands of points along the fiber length. They are also secure for using in explosive and inflammable environment. All these advantages stimulated a growing interest for applications in different areas for structural health monitoring, leak detection in oil and gas industry, etc.

In recent years, an increasing activity was demonstrated in development of techniques suitable for intrusion detection and localization, distributed acoustic and vibration sensors. Most sensitive optical techniques for detection of small dynamic perturbations are based on interferometric methods [1].

Many simple cost-effective fiber-optic systems utilizing coherent CW light sources and different combinations of interferometers (Sagnac, Mach-Zehnder, etc.) were proposed for distributed detection and localization of external disturbances [2–5]. Such systems are simple and inexpensive, however they possess a significant disadvantage. Only a single perturbation can be localized with an acceptable accuracy. For detection of 3 simultaneous disturbances and their independent location, a more complex system based on a dual-wavelength, dual-Sagnac architecture has been reported [4].

Phase-Sensitive OTDR technique [6] utilizes the Rayleigh scattering of coherent light pulses in a single-mode optical fiber and direct light detection. Due to interference of multiple light waves returned from a randomly distributed Rayleigh scattering centers, a single-pulse OTDR trace represents a speckle-like profile where amplitude of the photodetector signal is a random function of time/distance. For unperturbed fiber, the speckle-like OTDR traces are repeatable from pulse to pulse if the optical frequency of the probe light is well stabilized. A local perturbation of the sensing fiber modifies phase relations between waves backscattered in proximity of a perturbation point by a spatially-resolved segment of the optical fiber. It results in variation of light power returned back from the perturbed section of the fiber whereas for the unperturbed fiber sections the speckle-like trace remains stable. The phase-sensitive OTDR signal processing algorithm is looking for fast changes of the amplitude of the backscattered signal using accumulated consecutive traces, for each resolved segment of the fiber (for each speckle in the trace). Variation of the signal amplitude from pulse to pulse at some points of the OTDR traces is a sign of dynamic perturbations at the corresponding positions along the fiber.

Phase-sensitive OTDR allows detection of multiple simultaneous perturbations along the sensing fiber. Its configuration is relatively simple and is similar to a conventional OTDR. However, the interrogating laser must provide coherent light pulses with a very high contrast in order to mitigate a noisy coherent light pedestal. Usually, probe pulses are formed from a CW light of a coherent seed laser with help of high extinction ratio (>40 dB) electro-optic intensity modulators or fast high-contrast acousto-optic modulators [7,8]. Such modulators are expensive and require special controllers for temperature independent operation.

Much of research activity was devoted to increase the maximum sensing range of phase-OTDR which is limited to ~25 km by onset of non-linear effects such as Modulation Instability and Self-Phase Modulation in single-mode fibers [9,10]. Sensor systems based on conventional pulsed regime of operation and employing a coherent heterodyne detection as well as distributed Raman and Brillouin probe light amplification were demonstrated with sensing distances over 100 km [7–15]. However, such systems are much more complex and expensive.

There are well known optical reflectometry techniques using long probe signals without sacrificing a spatial resolution. Two techniques, namely Optical Frequency Domain Reflectometry (OFDR) [16,17] and Correlation OTDR [18] can be useful for distributed detection of dynamic perturbations.

Recently, a dynamic Optical Frequency Domain Reflectometry system was reported for distributed acoustic sensing. The proposed system is based on a CW ultra-coherent fast tunable laser and coherent detection scheme [19]. The method can provide high spatial resolution and sensitivity. However, for detection of dynamic perturbations in a sensing fiber of 10 km, a signal acquisition rate of 250 MSamples/s was required even for spatial resolution of tens of meters, since the maximum signal frequency is determined by the maximum length of the sensing fiber and by the scanning rate of the laser.

In correlation reflectometry, a lightwave with a random power fluctuation is used as a probe signal [20,21] and the returned from the fiber signal is compared with the probe signal. The bandwidth and the randomness of probe signals are key parameters determining overall performances of the correlation OTDR. Assuming that the autocorrelation function of the probe signal can be approximated by the delta function, the impulse response of the optical fiber can be recovered by calculating cross-correlation between the probe signal and the signal backscattered from the fiber. The width of the autocorrelation peak of the probe signal determines the system spatial resolution.

Different methods for generation of random probe optical signals were proposed and experimentally demonstrated. The most common method is based on modulation of laser light with special pseudo-random code sequences. To be useful for interferometric detection of perturbations with coherent lasers, digital coding techniques require using of high-extinction

ratio external optical modulators, fast code generators and therefore can be even more complex in comparison with a simple phase-OTDR. Another approach to generate optical random probe signals is based on laser sources operating in quasi-continuous regime. A semiconductor laser with an external optical feedback operating in chaotic regime was used for generation of random intensity modulated light with the bandwidth of up to 20 GHz. A high resolution correlation OTDR was demonstrated using such a random laser [22]. However, an external optical feedback introduces a photon round-trip period which results in appearance of lateral periodic side-lobes in the autocorrelation function. Recently, a correlation OTDR with a sensing distance of 100 km and 8.2 cm spatial resolution was reported [23]. It is based on a fiber super-continuum light source. However, the coherence length of these sources is not sufficient for interferometric sensors. In our previous works we presented a correlation OTDR for interrogation of multiplexed FBG sensors with ultra-low reflectivity, as low as 0.005%, for static measurements as well as initial results for interferometric detection of dynamic perturbations [24,25].

In this work we present a detailed description of a simple phase-sensitive correlation OTDR employing a free-running telecom-grade DFB diode laser as a light source without any external modulator for generation of a random probe signal. We discuss a principle of operation of the sensor and present results on a proof-of-concept demonstration of the sensor functionality.

2. Principle of operation and experimental setup

Usually, the phase noise of a laser light plays a destructive role in coherent optical systems reducing signal-to-noise ratio. An influence of phase noise on performance of interferometric systems were analyzed in many works, see for example [26,27]. Recently, an interesting results on random number generators based on measurement of a phase noise of a laser were presented [28,29]. An unbalanced fiber Mach-Zehnder interferometer was used to generate truly chaotic intensity signals. The true randomness of the quantum phase noise of a laser originates from the random nature of spontaneous emission. A very long continuously generated random bit sequence with length of 14 Gbit was demonstrated satisfying all standard randomness tests. The quantum phase noise is laser-power-dependent and determines the line shape and line width of the laser light. The linewidth experiences broadening with decreasing of the laser output power [30]. Close to the lasing threshold, the quantum phase noise can dominate over technical factors of the phase noise and can provide significant broadening of the laser emission spectrum. Such properties make the quantum phase noise of laser light very interesting for applications in fiber-optic sensors.

In correlation based OTDRs, there exists a tradeoff between the coherence length of the interrogation light and the spatial resolution. By selecting proper parameters of the light source, distributed interferometric sensors for detection and localization of dynamic perturbations can be interrogated utilizing a CW laser. The technique described here, unlike conventional pulsed phase-sensitive OTDRs, does not need any short-pulse sources or light intensity modulators, but it uses free-running unmodulated CW DFB laser whose natural phase noise is converted into random intensity modulation with a help of unbalanced two-beam interferometer.

In configuration with unbalanced interferometer, the random reference signal is produced due to interference of the laser light possessing a phase fluctuation with its delayed replica. As it is known, the resulting statistical properties of light power at the interferometer output, such as mean power value and its variance depend on time delay introduced by the interferometer [26,27]. The variance of light power defines the power of a probe signal and finally the amplitude of the correlation signal. If we consider interference of two replicas of the laser light with a unit power each and the coherence time, τ_c , the normalized mean

power, \bar{I} , and the variance of the light power, σ_I^2 , at the output of the interferometer can be described by

$$\bar{I} = 2 \left[1 + e^{-\frac{|\Delta t|}{\tau_c}} \cos \theta \right], \quad (1)$$

$$\sigma_I^2 = 2 \left[1 - e^{-\frac{2|\Delta t|}{\tau_c}} (1 + \cos 2\theta) + e^{-\frac{4|\Delta t|}{\tau_c}} \cos 2\theta \right], \quad (2)$$

where Δt is a delay time, θ is a product of the light wavenumber and the optical path difference of the interferometer, it represents a phase difference at a given wavelength of the laser light at the output of the unbalanced interferometer. Figure 1 shows calculated results for standard deviation and mean value of the output light power as a function of the time delay in fractions of τ_c for different phase delay angles θ . As one can see from Fig. 1(a), when the OPD of the interferometer exceeds 3 times the coherence length of the laser light the variance (probe signal power) gets its maximum value and this value does not depend on the phase angle θ . At the same time, for sensing interferometers with delays shorter than the light coherence time, high contrast interferometric fringes (variation of the mean light power between values corresponding to $\theta = 0$ and $\theta = \pi$) can be observed, see Fig. 1(b). These two properties of the laser light undergoing a phase fluctuation can be useful for a phase-sensitive correlation reflectometer.

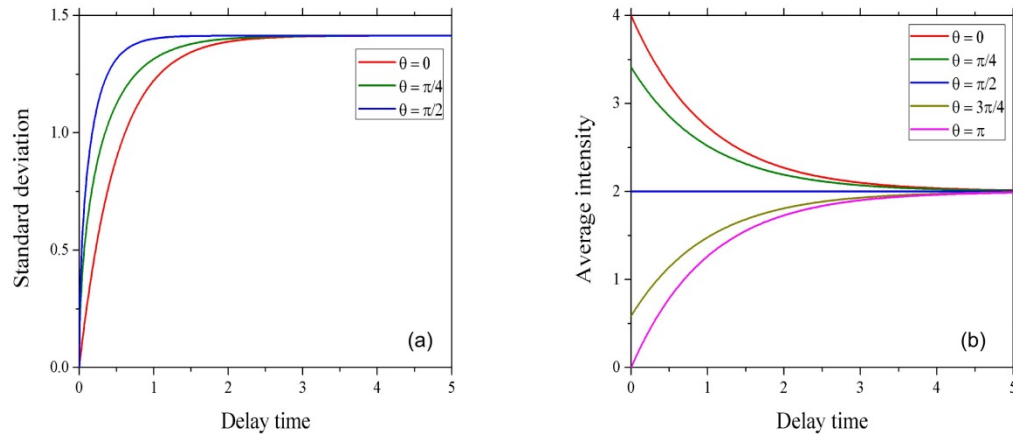


Fig. 1. Evaluation of the standard deviation (a) and average light intensity (b) at the output of the unbalanced interferometer in presence of the laser quantum phase noise. Delay time is presented in terms of coherence time of the laser light.

The experimental arrangement of the sensor is represented in Fig. 2. As a light source we used a standard telecom DFB diode laser with a simple pump current controller operating in CW mode. A laser diode temperature controller was used to stabilize the output light frequency. We used the additional optical isolator to avoid any intensity instabilities which can be induced due to strong back-reflections into the laser cavity. In semiconductor lasers, the phase noise determines the laser output bandwidth, and so the coherence length of the laser light [30]. In order to generate a probe signal with random intensity variations, we used an interferometer with optical path difference (OPD) of 200 meters. The interferometer optical pass difference was selected to be longer than the coherence length of the laser light.

That provides a maximum power of a random probe signal with a power level independent of OPD variations with temperature.

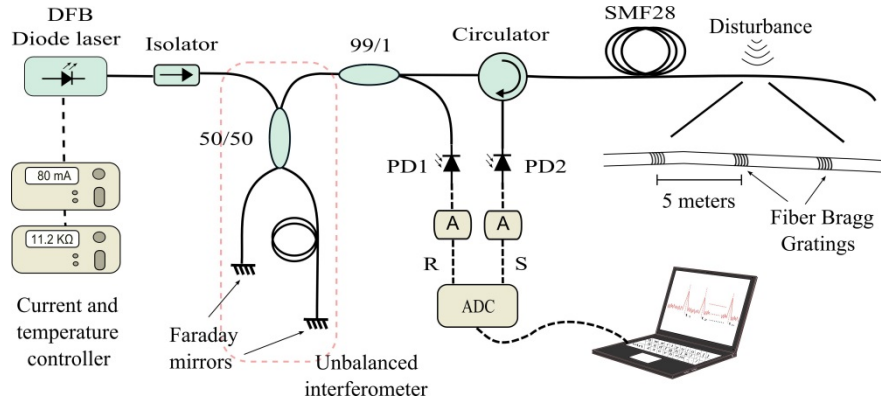


Fig. 2. Experimental set-up of the phase-sensitive correlation OTDR. (A: AC-coupled trans-impedance amplifiers; ADC: 2-channel Analog-to-Digital Converter PC board).

The laser emission, after passing through the fiber optic isolator is divided by 3 dB coupler in two arms of unbalanced interferometer. The two Faraday mirrors were used to increase the light power at the interferometer output and to avoid fluctuations of the probe signal power due to temperature-dependent polarization fading. Light coming from the interferometer is divided by 1/99 fiber splitter in two channels, the reference and the measurement ones. The AC-coupled photo-detectors in the reference and signal channels were identical (bandwidth of 10 MHz). In the reference channel, an additional attenuator was used to get light power at the reference photo-detector PD1 to be approximately similar to power level returned from the sensing fiber to the signal photo-detector PD2. It was done in order to utilize the same gain of amplifiers and thus to avoid a possible mismatching in transfer functions of the electronic channels. The level of optical power coupled into the sensing fiber through the fiber-optic circulator was of 0.3 mW. The laser operated at reduced pump level in order to reduce its coherence length. The laser wavelength was stabilized at 1535 nm, the FWHM bandwidth of the reference signal was of 5 MHz and the estimated coherence length of the laser light was approximately 20 meters in vacuum. The sampling rate of the ADC board was of 25 MHz. That corresponds to sampling distance interval of 4 m. Correlation functions were calculated utilizing the Fourier-transform-based algorithm. The length of captured realizations of reference and sensor signals was of 512 samples. Signal acquisition and processing were performed in LabView. It takes approximately 3ms for calculation of cross-correlation function using a PC. So, the sampling rate for perturbation detection was of 300 Hz in our experimental setup. It was sufficient for demonstration purposes. Further optimization of the signal processing can increase the sensor performance.

The OTDR traces were obtained by calculating the cross-correlation of signals from photo-detectors PD1 and PD2 in the reference and back-reflected channels. A calculated correlation function thus represents distribution of reflectivity along the optical fiber at the probe wavelength. The spatial resolution of our phase-sensitive correlation OTDR is determined by the coherence length of the laser which is proportional to the width of the autocorrelation function of the signal from the reference channel. Any two retro-reflectors separated by a fiber section shorter than the half of coherence length will perform as an interferometer. In the correlation trace, the response of such an interferometer will be represented by a single peak whose amplitude depends on phase delay between the reflected waves. Thus, perturbation of the fiber effective refractive index between adjacent reflectors will result in variation of the amplitude of the corresponding correlation peak. Dynamic

perturbations can be detected and localized by monitoring for fast variations of correlation amplitude in the correlation OTDR traces.

An example of probe signal captured with the reference photo-detector PD1 is shown in Fig. 3(a). Figure 3(b) represents the autocorrelation function calculated for a realization of the reference signal. As one can see in Fig. 3(b), the autocorrelation function of the probe signal is a narrow delta-function-like peak with a low level of side-lobes. At the -10 dB level, the autocorrelation peak width is approximately $0.2 \mu\text{s}$, that corresponds to the fiber length of 20 meters.

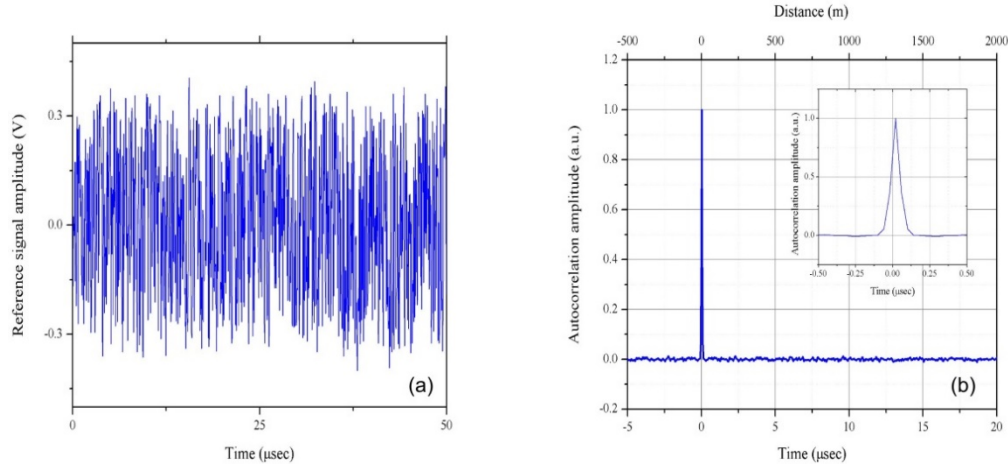


Fig. 3. (a) An example of the reference signal captured with AC-coupled photodetector; (b) Auto-correlation function calculated for the reference signal (inset: the central part of the autocorrelation function).

3. Results

Because of low fiber-coupled power of the DFB laser, for laboratory verification of the sensor functionality, we utilized a serial array of ultralow-reflectivity FBGs with distances between adjacent gratings shorter than the coherence length of the laser light. In experiments, 12 identical FBGs were written with an interval of 5 meters at the far end of SMF28 fiber with length of 1080 m, within a section located between 1015 and 1070 meters. Each grating had reflectivity of approximately 0.01% at the Bragg wavelength of 1535 nm and bandwidth of 0.3 nm. The gratings were written in the pristine SMF-28 fiber using a phase mask and small Nd:YAG laser operating at 4-th harmonic (266 nm) and producing 5 ns pulses with energy of 1 mJ. Each FBG was written with just 5 UV pulses.

Since the separation between adjacent FBGs is shorter than the coherence length of the laser source, the detected intensity signal was a result of interference of light waves reflected from a several adjacent FBGs. It means that correlation peaks of signals from the adjacent gratings are not resolved. Resulting correlation traces for the fiber section containing FBGs is represented by a superposition of the individual responses including interference components. It appears to be similar speckle-like traces in the conventional phase-sensitive OTDR. Figure 4 shows an example of the correlation trace obtained with only a single realization of the probe signal without averaging. A section containing FBGs is clearly visible on this trace.

For detection of dynamic perturbations, amplitudes of correlation traces were monitored for all resolved points along the fiber length. Each 3 milliseconds a correlation trace was obtained and time variation of the correlation amplitudes were plotted with this sampling period. In laboratory, we simulated dynamic perturbation by stretching the 0.5 meter long section of the fiber located at the distance of 1016 meters with a piezoelectric-transducer

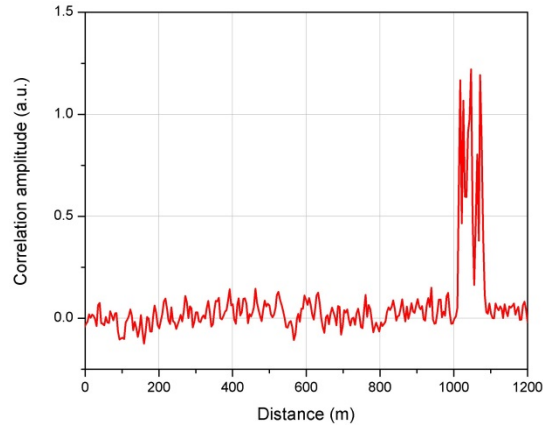


Fig. 4. Experimental cross-correlation trace for optical fiber with an array of 12 equally spaced FBGs in between 1015 and 1070 meters.

between the first and the second FBGs. No perturbation was applied to any FBG. Figure 5 demonstrates experimentally obtained time variation of amplitudes of the cross-correlation function measured for 4 different points along the sensing fiber. Figure 5(a) shows results for stable environmental

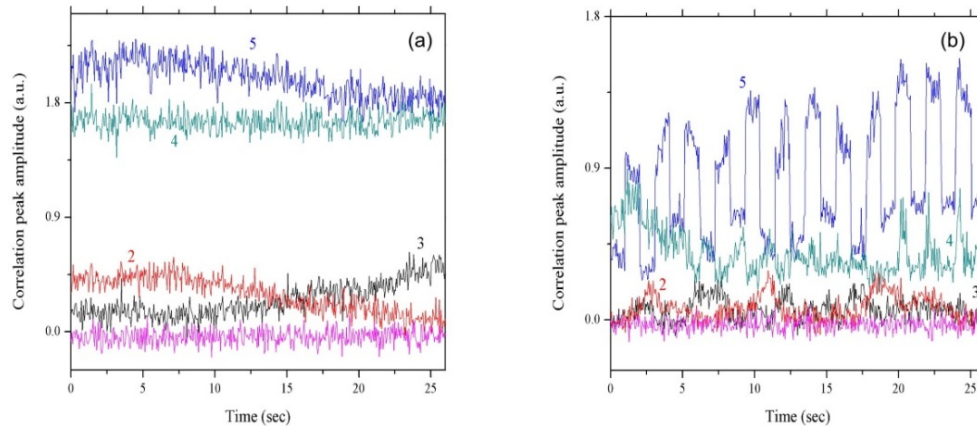


Fig. 5. Time variation of cross-correlation amplitudes measured at 4 different positions along the fiber (traces 2-5); (a) without an external mechanical perturbation; (b) a perturbation was applied at the distance of 1016 meters. Trace 1 represents the background level of the system noise, trace 2: measured at the distance of 500m; 3: at distance 710 m; 4: at distance 1050 m; 5: at distance 1016m where perturbation was applied. An array of FBG interferometers were formed in the fiber section from 1015 to 1070 meters).

conditions without an external perturbation. The traces 4 and 5 correspond to the fiber section containing the array of FBGs. The traces 2 and 3 correspond to the fiber sections without FBGs and most likely represent slow variations of speckles formed by Rayleigh backscattering. Slow variations of the signal amplitudes with time are attributed to effects of air flow and small temperature fluctuations. The trace 1 was measured for the distance longer than the fiber length, and, therefore indicates the system noise background. Figure 5(b) demonstrates the effect of an external perturbation. An electrical square-wave signal with a frequency of 0.5 Hz was applied to the piezoelectric transducer thus stretching the fiber. The peak-to-peak phase modulation of the 5-meter-long stretched interferometer was approximately 180° . The trace 5 represents a variation in time of the correlation amplitude at the distance corresponding to the point where a perturbation was applied to the fiber. One can

clearly see the detected signal. No additional signal processing was applied. The sampling period of traces presented in Fig. 5 was of 3 ms. Sharp changes of correlation amplitude in the trace 5 indicate that dynamic perturbations with bandwidth of up to 100 Hz can be detected. The correlation trace 4 obtained for the point located at 1050 m (which is 34 meters away from the point of perturbation) shows small fluctuation correlated with the applied perturbation. Such a behavior can be attributed to cross-talk effects because of partial overlapping of cross-correlation peaks corresponding to different interferometers separated by 34 meters. In our experiments, FBGs are not used as separate point sensors but rather to simulate the interference from weak reflections in a distributed sensor. The result of the interference from the several FBG reflections having random phase has a stochastic nature. The response from the mechanical perturbation, in average, decays exponentially with increase of the interferometer length containing the point of perturbation, according to the shape of the cross-correlation function. The cross-talk effect observed in the correlation trace 4 might appear due to random constructive interference of the light reflected by several interferometers containing the perturbed section of the fiber.

Figure 6 shows waterfall plot for the entire length of the sensing fiber obtained for the same experimental conditions as presented in Fig. 5(b). Green arrows with numbers at the right indicate positions along the fiber where corresponding traces were measured. A signal corresponding to external perturbations (trace 5) can be clearly seen at the distance of 1016 m where the piezoelectric actuator was activated. Within the range from 0 to 1000 m corresponding to the fiber section without FBGs, the waterfall plot demonstrates speckle-like traces with low amplitudes. These speckle patterns most likely are formed due to Rayleigh backscattering. Slow fluctuations of correlation amplitudes with time can be explained by influence of very small temperature variations and airflow in the laboratory room resulting in phase changes of interfering waves. During the first 19 seconds, a few fast changes in distribution of speckles occurred synchronously over the whole length of the grating-free fiber segment (some moments are indicated by red arrows), whereas in a period between 20 and 26 seconds no one such event occurred. We attributed this effect to a small but fast change of the DFB diode laser central frequency. From data presented in Fig. 5 and Fig. 6, for this preliminary experiment the location resolution can be estimated to be about 30 meters. This value is acceptable for some applications, such as, for example, intrusion detection and localization systems, etc.

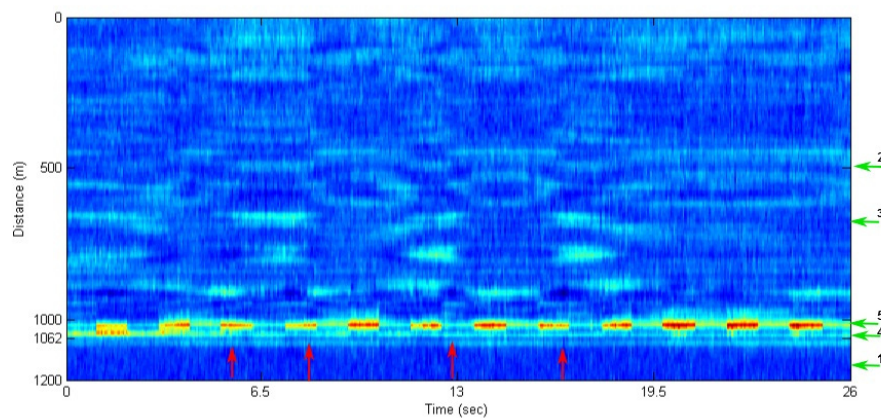


Fig. 6. Waterfall plot for the full length of the fiber. An amplitude of the cross-correlation is presented in pseudo-colors; the red color corresponds to maximum signal amplitude. Green arrows at the right indicate positions where traces 1-5 shown in Fig. 5(b) were measured. Red arrows at the bottom indicate some of the moments when, as we suppose, the laser central optical frequency suddenly slightly changed.

Operation of the proposed method was demonstrated using an array of ultra-weak reflectivity FBGs written in pristine SMF-28 fiber. Such gratings can be imprinted in SMF-28 fiber in a cost effective way through the protective polymer coating. Our experiments have shown that such ultra-low reflectivity gratings written in the SMF-28e fiber have sufficient thermal resistance and can operate in the full temperature range of the SMF-28e fiber. Nevertheless, increasing of fiber-coupled power and using a simple Er-doped fiber amplifier, operation of the proposed technique could be extended to standard single-mode fibers using just Rayleigh backscattering.

4. Conclusion

We presented a new phase-sensitive correlation OTDR suitable for detection and localization of multiple dynamic perturbations in single mode optical fibers. The system is very simple in configuration. It utilizes the quantum phase noise of laser light for generation of random coherent probe signals. The sensor uses a low-cost free-running DFB diode laser operating in CW regime with a fiber-coupled light power of about 1 mW. Detection and localization of dynamic perturbations was experimentally demonstrated. We believe, the proposed technique could be a basis for development of a cost-effective phase-sensitive correlation OTDR, especially for distances up to several kilometers.